Engineering Innovations
ISSN: 2813-1002, Vol. 9, pp 23-30
doi:10.4028/p-1BMxJg

Submitted: 2023-06-26
Revised: 2023-10-04
Accepted: 2023-10-04
Online: 2024-02-12

Cathodized Stainless Steel Mesh for Binder-Free $NiFe_2O_4$/NiFe Layer Double Hydroxides Oxygen Evolution Reaction Electrode

Natthapon Sripallawit[a] and Soorathep Kheawhom[b*]

Research Unit of Advanced Materials for Energy Storage, Chulalongkorn University, Bangkok 10330, Thailand

[a]6370081821@student.chula.ac.th, [b]soorathep.k@chula.ac.th

Keywords: Electrocatalyst; Oxygen evolution reaction; Cathodization

Abstract. Oxygen evolution reaction (OER) is an essential reaction commonly applied in various energy storage and conversion technologies. One of the common issues of OER lies in its low kinetic activity. Therefore, developing durable, low-cost, and high-performance OER catalysts is critical. Recently, many attempts have used stainless steel mesh (SSM) as the substrate for OER electrodes because SSM is abundant, cheap, and durable. Nickel/iron-based materials, i.e., $NiFe_2O_4$/NiFe layer double hydroxides (LDHs), are regarded as one of the most excellent OER catalysts in alkaline electrolytes, making them attractive low-cost materials for OER catalysts. However, synthesizing $NiFe_2O_4$/NiFe LDHs directly on the surface of SSM is challenging. Modifying the SSM surface through cathodization has proved to enhance the adhesion and OER activity. Moreover, the cathodization technique is facile and cost-effective. In this work, the surface of SSM is modified by cathodization treatment. Subsequently, $NiFe_2O_4$/NiFe LDHs are deposited onto the surface of treated SSM via a low-temperature one-step chemical bath deposition technique. This synthesis is a binder-free method; the resulted electrodes show excellent OER performance without the binder effects. The as-prepared electrodes have a small Tafel slope of 125.4 mV/dec (1 M KOH) and high durability (10 mA/cm^2 for 50 hours).

Introduction

Due to the obvious rising demand for energy, the demand for technology related to energy conversion and storage is increasing [1, 2]. As a result, the development of efficient, cost-effective, and sustainable renewable energy technology is important. Lithium-ion batteries are now widely employed in a variety of applications, including mobile phones, laptops, and electric vehicles, and they have almost dominated the rechargeable battery market. However, lithium-ion batteries' development and applications have been hampered by their low energy density (<350 Wh/kg), limited lithium resources, and safety concerns [3, 4].

Metal-air battery is one of the more intriguing batteries. since the reactants (O_2) are not kept in the cell but retrieved from the environment, the energy density of metal-air batteries is substantially higher than that of lithium-ion batteries [5]. Metal anodes for metal-air batteries come in a variety of materials, including lithium (Li), magnesium (Mg), aluminum (Al), zinc (Zn), and iron (Fe). Zn–air batteries (ZAB) have risen to the forefront of current rechargeable battery development due to their many advantages, such as: zinc is abundant in nature, has low toxicity, is extremely stable, can be handled safely in oxygen and humid environments, is economically priced, and is safe to use with aqueous electrolytes. Furthermore, gadgets made of zinc have a high specific and volumetric energy density [3, 6, 7]. Although Li-air batteries have the highest specific energy density, they are unstable when exposed to oxygen or water, necessitating an inert atmosphere and the use of organic electrolyte systems, which adds to the manufacturing complexity and safety issues. The safety concerns arise from the explosive reactivity of lithium with air or water, as well as the flammable organic electrolyte. Another disadvantage of Li-air batteries is that they are unsuitable for commercial application due to their high cost and limited lithium resources [3, 4].

However, ZABs still require improvement in the oxygen evolution reaction (OER) and oxygen reduction reaction (ORR), which occur during the charge and discharge processes [8, 9]. The problem with OER is that it has inert kinetics as it relates to the occurrence of four sequential electron transfers and the formation of an oxygen-oxygen bond [10, 11]. As a result, the use of a catalyst is required. Many studies have shown that iridium dioxide (IrO_2) and ruthenium dioxide (RuO_2) are highly efficient OER electrocatalysts in alkaline electrolytes, but the problem with precious metals is their low natural reserves and high cost [12]. Most catalysts are prepared in powder form, which requires a polymer binder to help the catalyst bind to a conductive substrate. The binders may deteriorate from continuous cycling and from the formation of O_2 gas bubbles during the OER reaction, resulting in catalyst detachment and dramatically decreased battery lifespan [3]. Based on the aforementioned problems, efforts were made to design a well-performed, inexpensive, and binder-free OER electrode.

Nickel/iron-based materials are regarded as one of the most excellent OER catalysts in alkaline electrolytes, making them one of the attractive low-cost materials as catalysts [13, 14]. As a result, numerous investigations have concentrated on the synthesis of nickel/iron-based electrocatalysts. Layered double hydroxides (LDHs) are great suggestions among them as high-performance catalysts because they have many advantages, such as having a large number of active sites and a large specific surface area [12]. At present, there are many research that use stainless steel mesh (SSM) as the substrate of electrodes because SSM is an easy-to-find, cheap, and durable material. There are also reports that it can increase the OER activity of SSM by improving its surface. Examples of interesting surface improvements are thermal treatment and cathodization treatment. Improving its surface through cathodization can increase OER activity, and this method is also very easy to implement [15].

In this work, we created electrodes from SSM that were surface enhanced by cathodization treatment and then coated with electrocatalysts to serve as OER electrode for ZAB with high efficiency and durability.

Experimental Section

Materials. Chemicals and Materials used in this work include stainless steel (304) 20 mesh was purchased from Lee Ngiab Seng (Thailand), Nickel (II) sulfate hexahydrate ($NiSO_4 \cdot 6H_2O$) was purchased from Kemaus, Iron (II) Chloride tetrahydrate ($FeCl_2 \cdot 4H_2O$) was purchased from Merck, Ammonia solution 25% (NH_4OH) was purchased from Loba Chemie Pvt. Ltd., Potassium hydroxide (KOH) was purchased from Kemaus.

Preparation of cathodized SSM. The SSM substrate (with dimensions of 1 cm × 1.5 cm) was ultrasonically cleaned in ethanol for 30 minutes. After that, it was cleaned with deionized water and then dried. The cathodization of SSMs was done utilizing a three-electrode setup and repetitive potential cycling, with SSM being used as the working electrode, platinum as the counter electrode, and Hg/HgO as the reference electrode. The cathodization method was carried out in -1.8 to 0.6 V (V vs. Hg/HgO), 0.1 M KOH electrolyte for up to 5 cycles at a scan rate of 10mV/s [15].

Preparation of $NiFe_2O_4$/NiFe LDH on cathodized SSM. Cathodized SSM were utilized as a substrate. The precursor solutions of 25 mL (0.05 M) $NiSO_4 \cdot 6H_2O$ and 25 mL (0.1 M) $FeCl_2 \cdot 4H_2O$ were transferred to a beaker, and the pH was adjusted to 10 by adding NH_4OH solution dropwise under vigorous stirring while the temperature was kept at 60 °C using a water bath. The cathodized SSM were submerged in the aforementioned solution for 2 hours, with the reaction bath temperature kept at 60 °C. Then the $NiFe_2O_4$/NiFe LDH on cathodized SSM were washed with deionized water multiple times and dried in a hot air oven at 75 °C for 1 hour [16].

Physical characterizations. The morphology and elements distribution of SSM surface was studied using field emission scanning electron microscopes (FE-SEM). The composition and

oxidation state of the synthesized $NiFe_2O_4$/NiFe LDH electrocatalyst was determined using x-ray photoelectron spectroscopy (XPS).

Electrochemical measurements. Squidstat plus was used to perform electrochemical measurements using a three-electrode system in the 1 M KOH electrolyte. Working electrodes were OER electrode samples, which had dimensions of 1×1 cm. Pt as the reference electrode, and KCl-saturated Ag/AgCl as the counter electrode. The OER activity was measured using linear sweep voltammetry (LSV) curves and Tafel slope is utilized to detect the rate-determining step in a four-electron-transfer process during oxygen evolution. The LSV measurements were performed with a potential range of -0.1 to 1.0 V vs Ref and a scan rate of 10 mV/s. Electrochemical impedance spectroscopy (EIS) was used on samples to acquire a better understanding of the OER kinetics, and it was performed from 1 Hz to 1000 kHz. In addition, the stability of the electrode was measured by a chronopotentiometry test and was conducted at 10 mA/cm^2 current density for 50 hours.

Results and Discussions

A FE-SEM characterization of pristine and cathodized SSM was performed to demonstrate that a treatment affects the surface morphology, as shown in Fig 1A, 1B. From FE-SEM image with a lowest magnification, it was not possible to clearly show the difference in the surface of SSM before and after treatment. When observing the high magnification, it is found that the SSM surface after cathodization has more irregularly shaped particles attached to the surface than ever before. Fig. 1C, 1D displays FE-SEM images of the electrocatalyst on pristine SSM and cathodized SSM. When observing $NiFe_2O_4$/NiFe LDH on cathodized SSM at low magnification, the electrocatalyst was found to have a thicker surface covering and formed higher than pristine SSM in some areas. At high magnification, both pristine SSM and cathodized SSM have the same electrocatalyst growth characteristics. The electrocatalyst that is on the pristine SSM and cathodized SSM was synthesized perpendicular to the surface as randomly bonded plates, and on those plates, it contained a lot of small spherical particles perched on it. Figure 2 shows x-ray photoelectron spectra of Ni 2p, Fe 2p, and O 1s for electrocatalyst. According to the results of XPS, Peak of Ni $2p_{3/2}$ and Ni $2p_{1/2}$ found that it was at positions 855.252, 856.199 and 872.915, 873.945 eV, respectively. These deconvoluted peak pairs relate to Ni^{2+} and Ni^{3+}, respectively. Next, Peak of Fe $2p_{3/2}$ and Fe $2p_{1/2}$ found that it was at positions 710.027, 711.709 and 723.776, 725.592 eV, respectively. These deconvoluted peak pairs relate to Fe^{2+} and Fe^{3+}, respectively. Next, deconvoluted peaks of O 1s with centers at 529.489, 531.060 eV are involved for metal oxides and hydroxides, respectively. The binding energies of nickel-ions, iron-ions and oxygen in this XPS spectra were proven the synthesis of the $NiFe_2O_4$/NiFe LDH film on cathodized SSM, in which it has peaks of Ni 2p, Fe 2p, and O 1s that well match the literature reports [16-17].

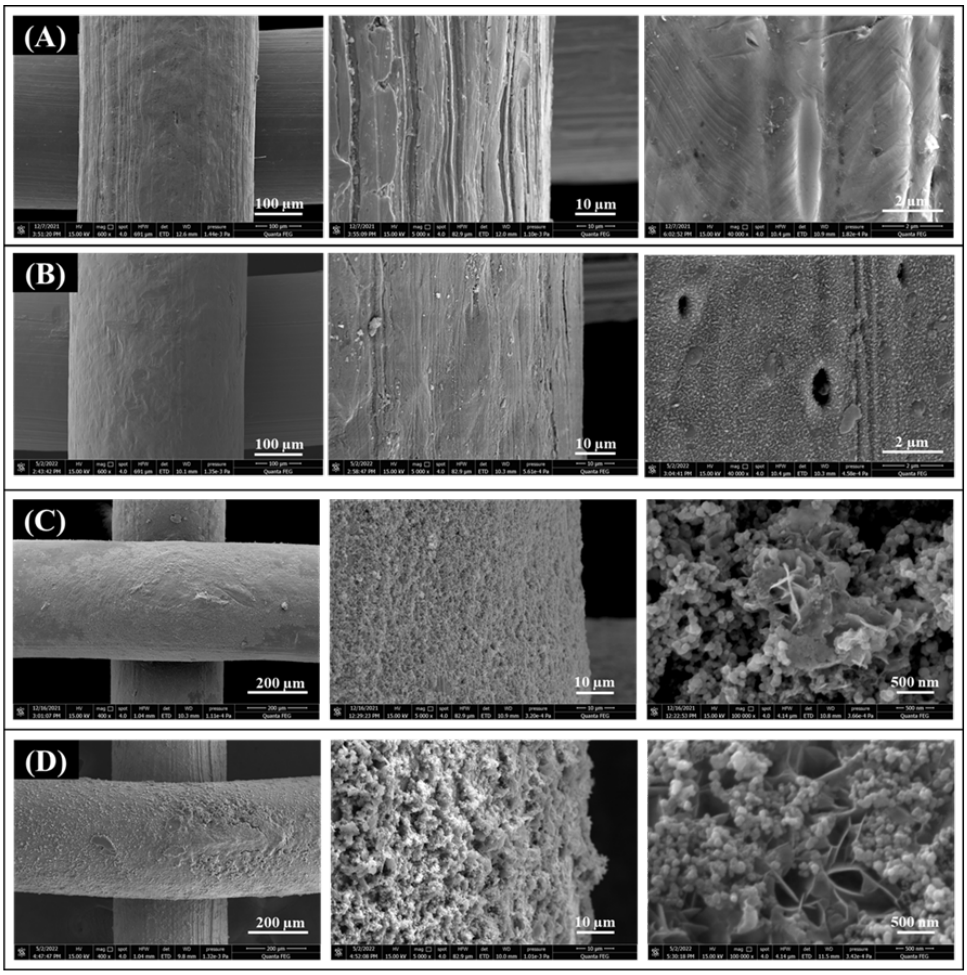

Fig. 1. Low- and high-resolution FE-SEM image for (A) pristine SSM, (B) cathodized SSM, (C) $NiFe_2O_4$/NiFe LDH on SSM, (D) $NiFe_2O_4$/NiFe LDH on cathodized SSM.

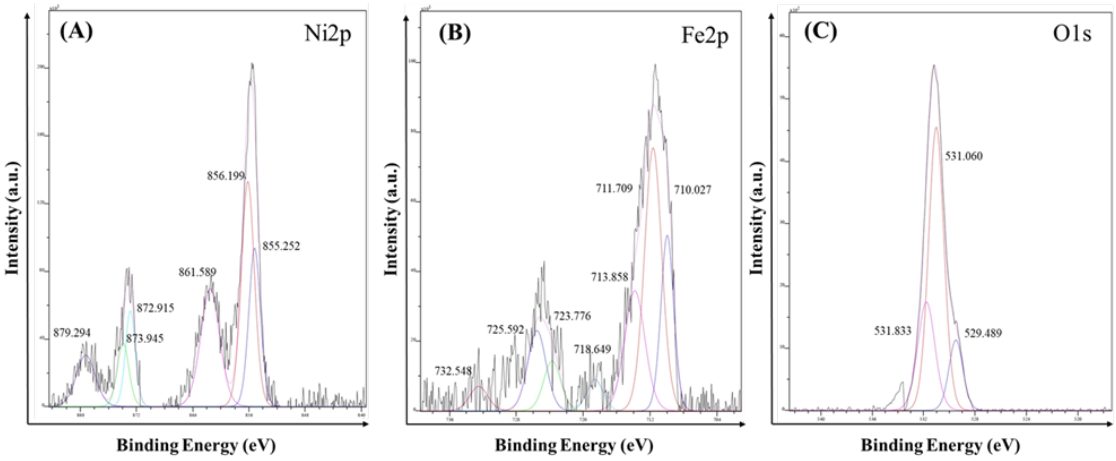

Fig. 2. XPS spectra of $NiFe_2O_4$/NiFe LDH on cathodized-no.4 SSM: (A) Ni 2p, (B) Fe 2p, and (C) O 1s.

A three-electrode setup in a 1 M KOH was used to assess the OER performance of the OER electrode. The LSV can show the difference in the OER activity of the samples. Fig. 3A shows the LSV curve comparison of bare SSM, $NiFe_2O_4$/NiFe LDH on SSM, and $NiFe_2O_4$/NiFe LDH on cathodized SSM. The best samples from all samples are $NiFe_2O_4$/NiFe LDH on cathodized SSM, it can be said that cathodization treatment results in a remarkable increase in OER activity. In addition, we have determined the Tafel slope of the bare SSM, $NiFe_2O_4$/NiFe LDH on SSM, and $NiFe_2O_4$/NiFe LDH on cathodized SSM shown in Fig. 3B. The result of calculating the Tafel slope of the SSM is

190.5 mV/dec, $NiFe_2O_4$/NiFe LDH on SSM is 171 mV/dec, and $NiFe_2O_4$/NiFe LDH on cathodized SSM is 125.4 mV/dec. As the results show, it can be interpreted that the $NiFe_2O_4$/NiFe LDH on cathodized SSM, showing a small Tafel slope, has the fastest electron transfer rate during oxygen evolution.

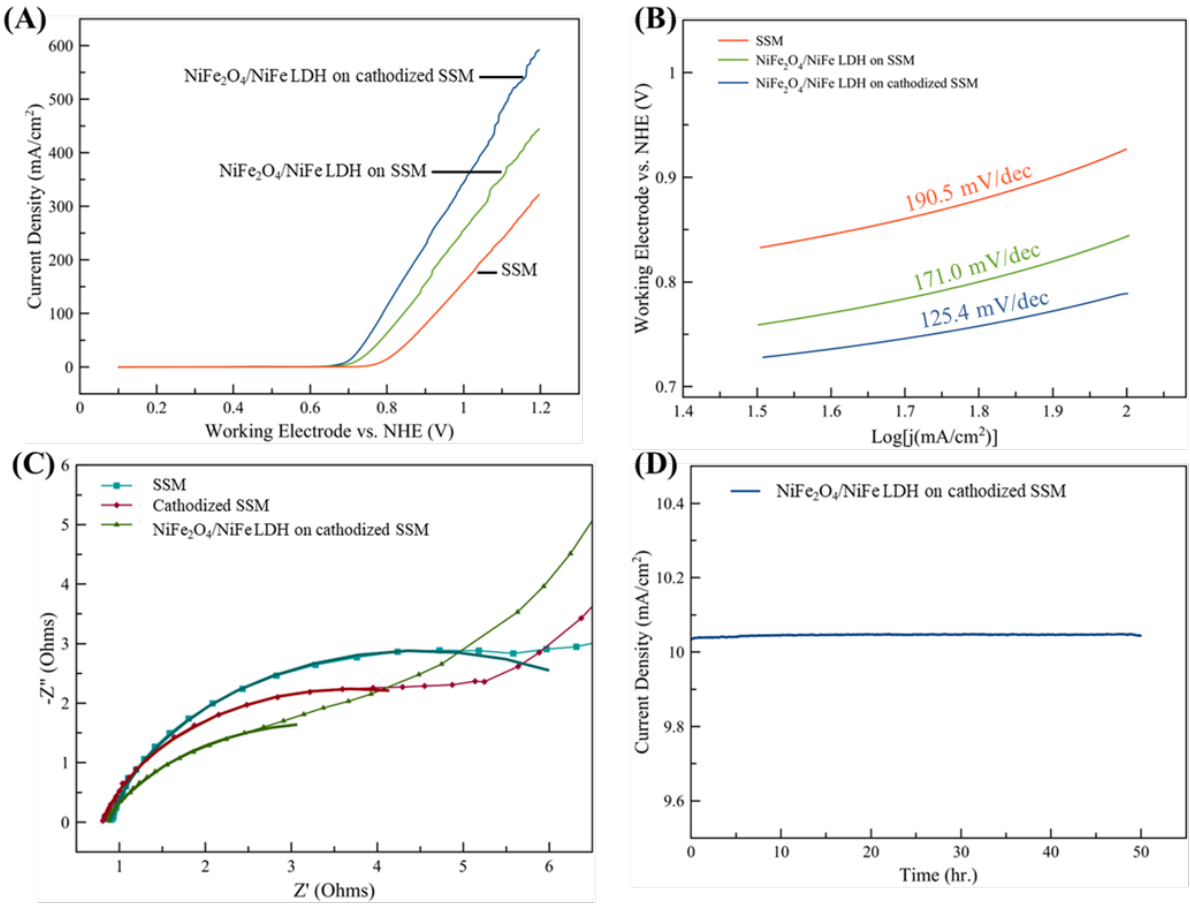

Fig. 3. Graphs of (A) LSV, (B) Tafel slope, (C) EIS, and (D) Chronoamperometric measurements.

The SSM that improves the surface with cathodization was found to have an electrocatalyst that grows higher on the surface than pristine SSM, possibly resulting in an even greater OER activity. In addition, the improvement of SSM surfaces with cathodization also causes OER active site ($Ni(OH)_2$ and NiOOH) to occur on the surface [15], which promotes increased OER activity.

Electrochemical impedance spectroscopy (EIS) was used to determine the behavior of electrode and electrolyte interfaces to obtain additional information about OER kinetics [15-16]. To assess stability, Chronoamperometric measurements were performed. In this work, the EIS and stability measurements were focused on the study of $NiFe_2O_4$/NiFe LDH on cathodized SSM, which has the best OER activity. Fig. 3C shows a Nyquist plots, that showed the OER kinetics improved when the SSM was improved with cathodization treatment. The charge transfer resistance (R_{ct}) for $NiFe_2O_4$/NiFe LDH on cathodized SSM (5.165 Ω) is lower than R_{ct} for bare SSM (7.193 Ω) and R_{ct} for cathodized SSM (5.856 Ω). This suggests that improving the surface of SSM by cathodization treatment and synthesis of the $NiFe_2O_4$/NiFe LDH to grow on its surface allows for greater charge transferability during OER, and when both methods are used together, it allows for a greater charge transfer than ever before. Fig. 3D shows chronoamperometry (i−t) curve of $NiFe_2O_4$/NiFe LDH on cathodized SSM at 10 mA/cm^2 for 50 hours and demonstrated the high stability of this sample.

We also investigated further on the morphology of the electrocatalyst after stability test. Fig. 4 shows the comparison between $NiFe_2O_4$/NiFe LDH on cathodized SSM before and after 50 hours of

stability testing and using the low- and high-resolution FE-SEM to see the electrocatalyst characteristics on the surface. At low magnification, it was found that the highly grown electrocatalyst was detached after testing, but the low-rise electrocatalyst remained well attached to the surface of the SSM surface. At high magnification, it was found that the characteristics of the electrocatalyst remained the same, with its morphology as a plate that rises perpendicular to the surface and is randomly connected, with small spherical particles on those plates.

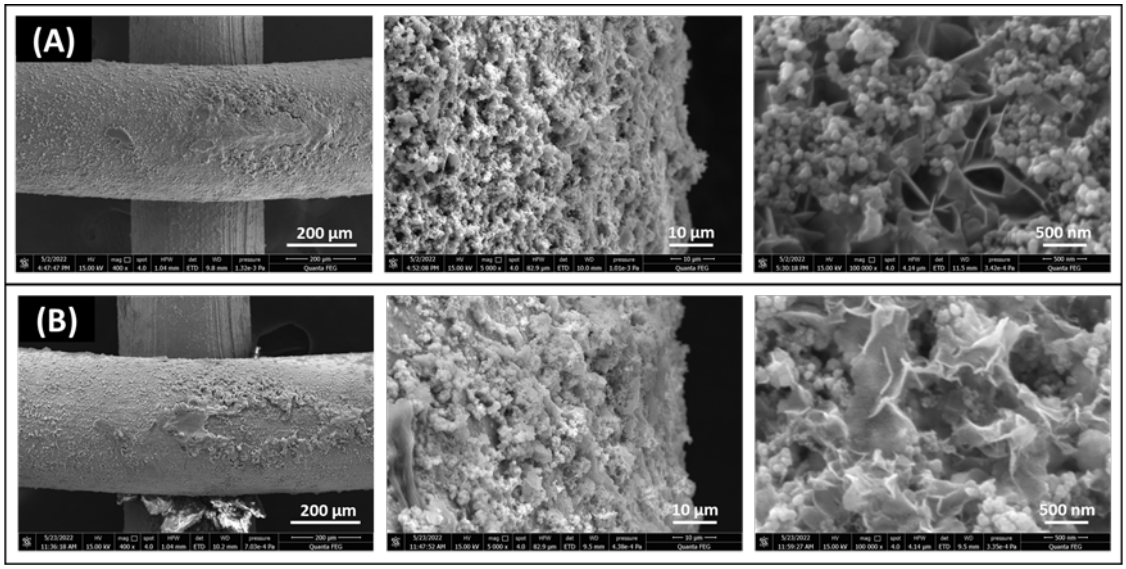

Fig. 4. Low- and high-resolution FE-SEM image for (A) $NiFe_2O_4$/NiFe LDH on cathodized SSM and (B) $NiFe_2O_4$/NiFe LDH on cathodized SSM after 50 hours of stability testing.

Fig. 5 shows a Nyquist plot of $NiFe_2O_4$/NiFe LDH on cathodized SSM after stability test at 10, 20, 30, 40, and 50 hours to confirm its stability, with the results from the figure showing that the $NiFe_2O_4$/NiFe LDH on cathodized SSM has constant OER kinetics for 50 hours. The charge transfer resistance (R_{ct}) of $NiFe_2O_4$/NiFe LDH on cathodized SSM after 10, 20, 30, 40, and 50 hours is 9.912 Ω, 10.66 Ω, 10.34 Ω, 10.45 Ω, and 10.22 Ω, respectively. Such results show that it has constant charge transferability and support the results of stability tests well.

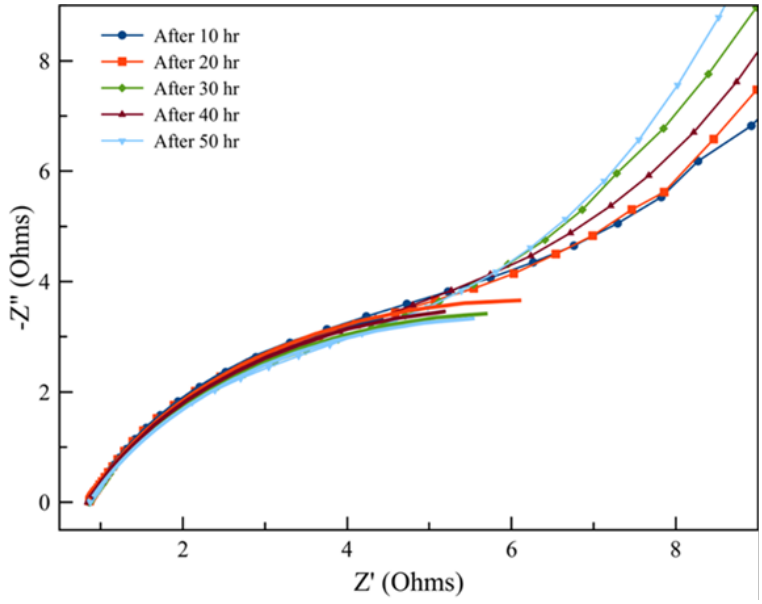

Fig. 5. EIS of $NiFe_2O_4$/NiFe LDH on cathodized SSM after 10, 20, 30, 40, and 50 hours of stability testing.

Conclusion

In this work, the effects of cathodization were studied for improving the surface of SSM to greater OER activity for air electrodes in zinc air batteries. The $NiFe_2O_4$/NiFe LDH was used as an electrocatalyst, in which it was coated on the surface of SSM samples by one-step chemical bath deposition technique. According to the results, $NiFe_2O_4$/NiFe LDH on cathodized SSM (Tafel slope = 125.4 mV/dec) has a greater OER activity than $NiFe_2O_4$/NiFe LDH on SSM (Tafel slope = 171 mV/dec). The results are due to the fact that electrocatalyst can deposit on the surface of the cathodized SSM, which is thicker than the surface of the pristine SSM, and the surface of cathodized SSM has a greater OER active site ($Ni(OH)_2$ and NiOOH). In addition, $NiFe_2O_4$/NiFe LDH on cathodized SSM also has high durability (10 mA/cm^2 for 50 hours). Therefore, SSM that improves the surface with the cathodized can be used as a better substrate for binder-free $NiFe_2O_4$/NiFe LDH oxygen evolution reaction electrode.

References

[1] J. Cho, S. Jeong, and Y. Kim, Commercial and research battery technologies for electrical energy storage applications, Progress in Energy and Combustion Science. 48 (2015) 84-101.

[2] M.S. Ghazvini1, G. Pulletikurthi1, T. Cui1, C. Kuhl1, F. Endres, Electrodeposition of zinc from 1-ethyl-3-methylimidazolium acetate-water mixtures: investigations on the applicability of the electrolyte for Zn-air batteries, Journal of The Electrochemical Society. 165(9) (2018) 354.

[3] X. Yan, Y. Ha, R. Wu, Binder-Free Air Electrodes for Rechargeable Zinc-Air Batteries: Recent Progress and Future Perspectives, Small Methods. 5(4) (2021) 2000827.

[4] J. Pan, Y. Xu, H. Yang, Z. Dong, H. Liu, B. Xia, Advanced architectures and relatives of air electrodes in Zn–air batteries, Advanced Science. 5(4) (2018) 1700691.

[5] X. Cai, L. Lai, J. Linb, Z. Shen, Recent advances in air electrodes for Zn–air batteries: electrocatalysis and structural design, Materials Horizons. 4(6) (2017) 945-796.

[6] K. Harting, U. Kunz, T. Turek, Zinc-air batteries: prospects and challenges for future improvement, Zeitschrift für Physikalische Chemie. 226(2) (2012) 151-166.

[7] B. Lee, H. Lee, H. Kim, K. Chung, B. Choa, S. Hyoung, Elucidating the intercalation mechanism of zinc ions into αMnO 2 for rechargeable zinc batteries, Chemical communications. 51(45) (2015) 9265-9268.

[8] T. Zhang, Z. Tao, J. Chen, Magnesium–air batteries: from principle to application, Materials Horizons. 1(2) (2014) 196-206.

[9] L. Ma, S. Chen, D. Wang, Q. Yang, F. Mo, G. Liang, N. Li, H. Zhang, J.A. Zapien, C. Zhi, Super-stretchable zinc–air batteries based on an alkaline- tolerant dual-network hydrogel electrolyte, Advanced Energy Materials. 9(12) (2019) 1803046.

[10] B. Zhang, X. Zheng, O. Voznyy, R. Comin, M. Bajdich, M. García-Melchor, L. Han, J. Xu, M. Liu, L. Zheng, F.G. de Arquer, C.T. Dinh, F. Fan, M. Yuan, E. Emre Yassitepe, N. Chen, T. Regier, P. Liu, Y. Li, P. De Luna, A. Janmohamed, H. L Xin, H. Yang, A. Vojvodic, E. Edward H Sargent, Homogeneously dispersed multimetal oxygen-evolving catalysts, Science. 352(6283) (2016) 333-337.

[11] L. Han, S. Dong, E. Wang, Transition-metal (Co, Ni, and Fe)-based electrocatalysts for the water oxidation reaction, Advanced materials. 28(42) (2016) 9266-9291.

[12] F. Liao, X. Zhao, G. Yang, Q. Cheng, L. Mao, L. Chen, Recent advances on two-dimensional NiFe-LDHs and their composites for electrochemical energy conversion and storage, Journal of Alloys and Compounds. 872 (2021) 159649.

[13] S. Niu, Y. Sun, G. Sun, D. Rakov, Y Li, Y Ma, J. Chu, P. Xu, Stepwise electrochemical construction of FeOOH/Ni (OH) 2 on Ni foam for enhanced electrocatalytic oxygen evolution, ACS Applied Energy Materials. 2(5) (2019) 3927-3935.

[14] M.B. Stevens, C. D. M. Trang, L.J. Enman, J. Deng, S.W. Boettcher, Reactive Fe-sites in Ni/Fe (oxy) hydroxide are responsible for exceptional oxygen electrocatalysis activity, Journal of the American Chemical Society. 139(33) (2017) 11361-11364.

[15] G. Zhang, L Shen, P. Schmatz, K. Krois, B. J.M. Etzold, Cathodic activated stainless steel mesh as a highly active electrocatalyst for the oxygen evolution reaction with self-healing possibility, Journal of Energy Chemistry. 49 (2020) 153-160.

[16] A.A. Kashale, C. Yi, K. Cheng, J. Guo, Y. Pan, I.P. Chen, Binder-free heterostructured NiFe2O4/NiFe LDH nanosheet composite electrocatalysts for oxygen evolution reactions, ACS Applied Energy Materials. 3(11) (2020) 10831-10840.

[17] Z. Cai, D. Zhou, M Wang, S. Bak, Y. Wu, Z. Wu, Y. Tian, X. Xiong, Y. Li, W. Liu, S. Siahrostami, Y. Kuang, X. Yang, H. Duan, Z. Feng, H. Wang, X. Sun, Introducing Fe2+ into nickel–iron layered double hydroxide: local structure modulated water oxidation activity, Angewandte Chemie. 130(30) (2018) 9536-9540.